U–Pb ages of detrital zircons from the Basal allochthonous units of NW Iberia: Provenance and paleoposition on the northern margin of Gondwana during the Neoproterozoic and Paleozoic

Rubén Díez Fernández [a,*], José R. Martínez Catalán [a], Axel Gerdes [b], Jacobo Abati [c], Ricardo Arenas [c], Javier Fernández-Suárez [c]

[a] Departamento de Geología, Universidad de Salamanca, 37008 Salamanca, Spain
[b] Institut für Geowissenschaften, Mineralogie, Goethe-Universität, D-60438 Frankfurt am Main, Germany
[c] Departamento de Petrología y Geoquímica and Instituto de Geología Económica, Universidad Complutense / Consejo Superior de Investigaciones Científicas, 28040 Madrid, Spain

Keywords:
NW Iberia
Variscan allochthonous terranes
Detrital zircons
LA-ICP-MS
U–Pb dating
Geodynamics

A B S T R A C T

LA-ICP-MS U–Pb ages of detrital zircons from eight siliciclastic samples from the Basal units of the Variscan allochthonous complexes of NW Iberia are used to establish the maximum depositional age and provenance of two tectonically-stacked metasedimentary sequences deposited on the outermost margin of Gondwana, and subsequently involved in the Rheic Ocean suture. The maximum depositional ages for the two sequences is latest Neoproterozoic and latest Cambrian, respectively. The age spectra are also used to discuss the paleoposition of the NW Iberian basement on the continental margin of Gondwana prior to the opening of the Rheic Ocean, which is tentatively placed in northern Africa, between the West African and Saharan cratons. Based on similarities and differences with age data from the NW Iberian autochthon and other allochthonous terranes involved in the Rheic suture, the relative proportions of Mesoproterozoic zircons in both assemblages are proposed as markers of proximity to the eastern part of the West African craton during late Neoproterozoic and late Cambrian. The geodynamic processes that took place along this part of Gondwana during the late Neoproterozoic, late Cambrian and Early Ordovician are discussed in the light of the LA-ICP-MS results, as well as the sedimentological record, magmatic evolution and plate tectonic setting of NW Iberia. These processes are linked to late Neoproterozoic and Cambro-Ordovician subduction events beneath the northern Gondwanan margin.

1. Geological setting

The allochthonous complexes of NW Iberia are a stack of nappes thrust over the sequences of the Iberian autochthon (Fig. 1a), which formed part of the northern margin of Gondwana for the entire Paleozoic (Martínez Catalán et al., 2007, 2009).

Three groups of allochthonous units have been distinguished (Fig. 1b and c). The Upper units, on top of the nappe pile, are pieces of a Cambro-Ordovician ensialic island arc (Abati et al., 1999, 2003; Andonaegui et al., 2002; Santos et al., 2002) inferred to have been detached from northern Gondwana by the roll-back of the subducting slab of the Iapetus–Tornquist ocean, to leave a new oceanic realm, the Rheic Ocean, in its wake (Stampfli and Borel, 2002; Stampfli et al., 2002; Winchester et al., 2002; von Raumer et al., 2003; Abati et al., 2010).

Relicts of oceanic floor form the middle allochthonous units, known as the Ophiolitic units, represent the suture of the Rheic Ocean (Díaz Garcia et al., 1999; Pin et al., 2002, 2006; Arenas et al., 2007; Sánchez Martínez et al., 2007) and possibly remnants of older oceanic domains (Sánchez Martínez et al., 2006; Sánchez Martínez, 2009).

The Basal units, at the base of the nappe stack, represent distal parts of the Gondwana continental margin. They preserve calc-alkaline igneous rocks roughly coeval with the Cambro-Ordovician suite of the Upper units (Abati et al., 2010), and experienced extension and rift-related magmatism during the Ordovician (Floor, 1966; Ribeiro and Floor, 1987; Pin et al., 1992), while the Rheic oceanic lithosphere was being created. Subsequently, the Basal units were subducted beneath Laurussia at the onset of Variscan collision (Arenas et al., 1995, 1997; Santos Zalduegui et al., 1995; Rodríguez et al., 2003; Abati et al., 2010), and exhumed by crustal-scale thrusting accompanied by recumbent folding and tectonic denudation during the Variscan Orogeny (Martínez Catalán et al., 1996, 1997; Díez Fernández and Martínez Catalán, 2009).

An imbricate thrust sheet, composed of siliciclastic sedimentary and volcanic rocks known as the Parautochthon, Lower allochthon or Schistose domain, separates the allochthonous complexes from the autochthon. The latter consists of a thick metasedimentary sequence which, as with the Lower allochthon and the Basal units, was deposited along the northern margin of Gondwana. The autochthonous sedimentary sequences of NW Iberia record the late Neoproterozoic and early

* Corresponding author. Tel.: +34 923 294488; fax: +34 923 294514.
E-mail address: georuben@usal.es (R. Díez Fernández).

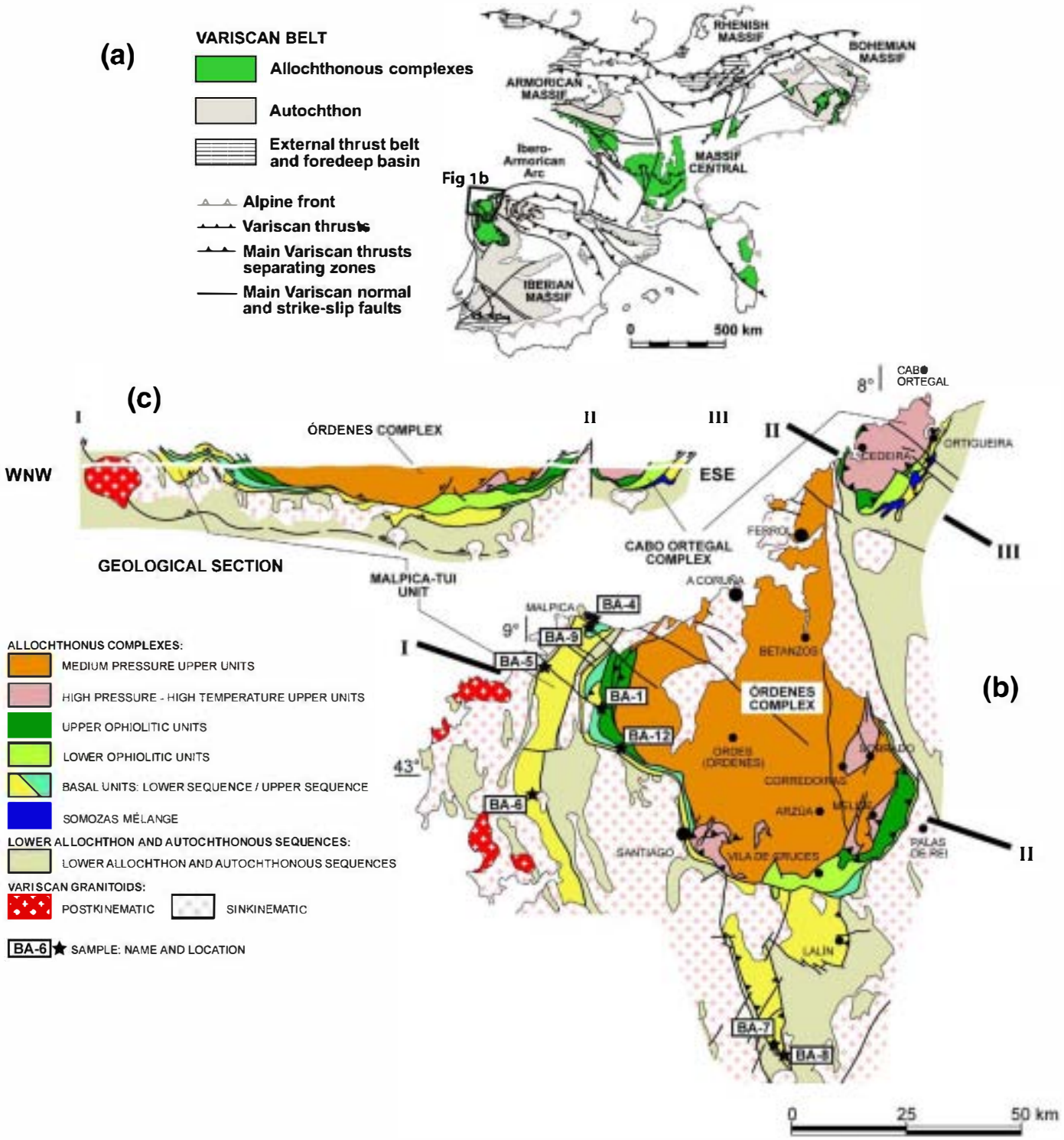

Fig. 1. (a) Location of the study area in the Variscan belt of Europe. (b) Map showing the allochthonous complexes of Órdenes, Cabo Ortegal and northern half of Malpica-Tui in Galicia, NW Spain, and the location of samples analyzed. (c) Representative cross section showing the general structure. Note the nappe stacking and the position of the Lower and Upper sequences. Top-to-the-ESE kinematics often represents thrusting, whereas top-to-the-WNW movement is related to extensional collapse and reactivation of previous structures.

Paleozoic evolution of the northern Gondwana margin, including the Avalonian–Cadomian active margin in the Neoproterozoic (Rodríguez Alonso et al., 2004), the development of a passive margin during the Cambrian, the Cambro-Ordovician opening of the Rheic Ocean, and the return to passive-margin conditions until the onset of the Variscan collision in late Devonian times (Martínez Catalán et al., 2007, 2009; von Raumer and Stampfli, 2008).

2. The stratigraphic succession of the Basal units

The Basal allochthonous units comprise two tectonically juxtaposed metasedimentary sequences (Fig. 1c), the Upper sequence representing a paleogeographic domain distinct from that of the Lower sequence. Both sequences were involved in the initial subduction that preceded Variscan collision, but the Lower sequence developed eclogite facies

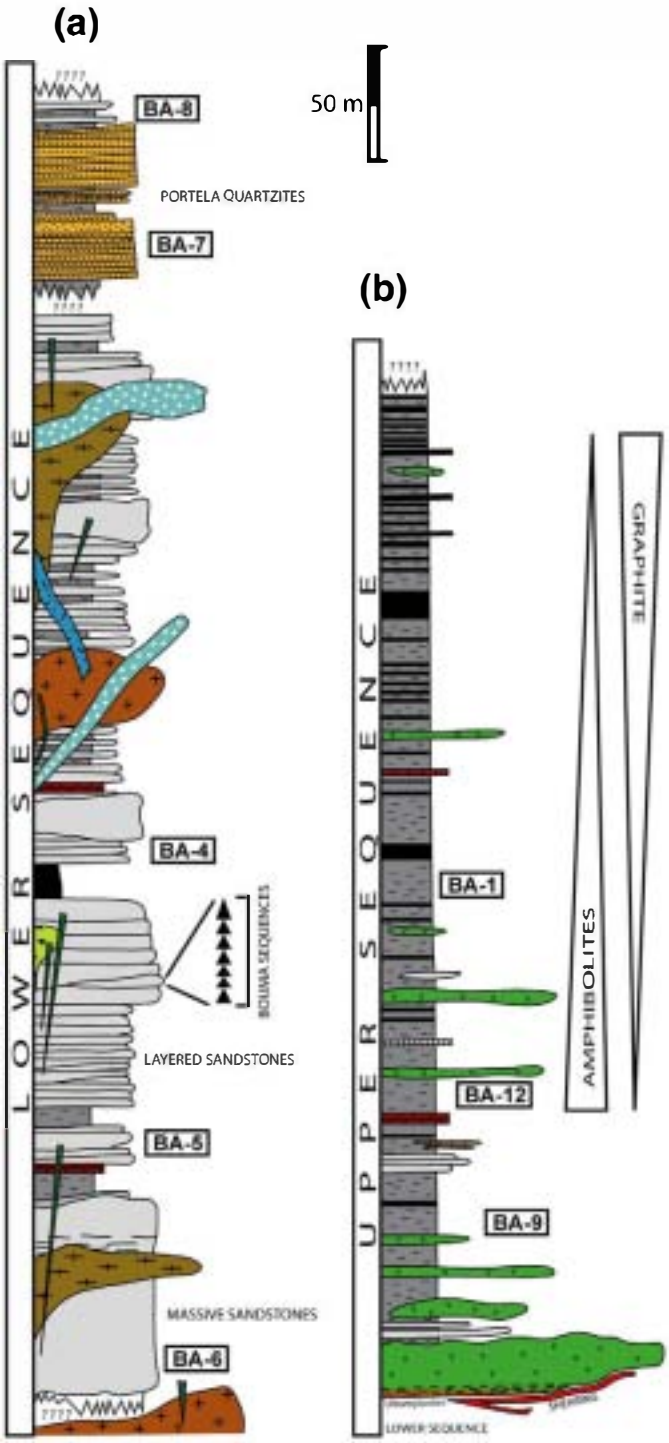

SEDIMENTARY-IGNEOUS // METAMORPHIC LITHOLOGIES

- Quartzitic sandstones // Quartzites
- Immature sandstones (greywackes) // Albite-bearing paragneisses
- Pelites - Semipelites // Albite-bearing schists
- Horizons enriched in organic matter // Graphite-bearing schists
- Limestones // Calc-silicate lenses
- Cherts // Metacherts

- N-MORB volcanics // Amphibolites
- Alkali basalts // Amphibolites - Eclogites
- Tonalitic granitoids // Eclogitic orthogneisses
- Granodiorites // Granodioritic gneisses
- Granites // Granitic gneisses
- Alkaline granites // Alkaline gneisses
- Peralkaline granites // Peralkaline gneisses

metamorphism (Gil Ibarguchi and Ortega Gironés, 1985) whereas the Upper sequence reached only blueschist facies conditions (López Carmona et al., 2010). The upper limit of the Upper sequence is a partly reworked thrust, and the original thrust contact between both sequences was also reworked during the Variscan orogenic collapse (Gómez-Barreiro et al., in review). However, differences between the two sequences occur not only in their metamorphic evolution but also in their litostratigraphy.

2.1. The Lower sequence

The strong heterogeneity of deformation in this sequence during the subduction and exhumation processes allows the original sedimentary stratigraphy to be characterized in the less deformed domains. These are preserved as meso- to macro-scale boudins that frequently reach map-scale size. The Lower sedimentary sequence consists of a thick, monotonous pile of immature sandstones (greywackes) alternating with minor layers or lenses of pelites, graphitic schist, calc-silicate layers and quartzites (Fig. 2a). The sandstones preserve Bouma sequences, crossed bedding, erosive contacts and normal graded bedding. They are clast-supported sedimentary rocks containing angular fragments of feldspars (the most abundant clasts), quartz and detrital micas in a clay-rich matrix with carbonaceous material. Pelitic horizons are common among the sandstones, and carbonaceous matter within them may become so abundant as to form graphitic horizons.

The sandstones form sequences up to 50 m thick. The normal thickness of the layers ranges from less than 1 dm to more than 1 m and often occur as a monotonous alternation of thin-bedded sandstones. The thicker the layers, the more massive the internal structure. No conglomeratic levels have been found, but it is possible to find grains bigger than 2 mm in the less deformed domains.

The quartzites (Portela Quartzites of Marquínez Garcia, 1984) occur relatively high in the sequence, and according to the restoration of Variscan structures made by Martínez Catalán et al. (1996), they lie in a paleogeographic position relatively close to the Gondwanan mainland.

In the moderately to highly deformed and metamorphosed areas, the sequence consists of albite-bearing schists and paragneisses alternating with centimetre-thick lenses of mica schists, graphite-bearing schists, and calc-silicate lenses, in which the sedimentary layering can still be seen.

Intruding the sediments are mafic dykes (alkali basalts; Marquínez García, 1984; Rodríguez, 2005), calc-alkaline granitoids (tonalites and granodiorites), and rift-related granitoids (alkaline to peralkaline and alkali-feldspar granites; Floor, 1966; Ribeiro and Floor, 1987; Pin et al., 1992), all transformed during the Variscan Orogeny into eclogites, amphibolites and orthogneisses (Rodríguez, 2005). The age of the oldest calc-alkaline orthogneisses (495–500 Ma; Abati et al., 2010) establishes a minimum depositional age for the Lower sequence.

The original thickness of the Lower sequence cannot be calculated because of the ductile deformation accompanying subduction, thrusting, recumbent folding and tectonic denudation. A minimum present thickness of 4 km can be estimated, but this value probably represents less than half of the original thickness.

2.2. The Upper sequence

No significant deformation partitioning is visible during the subduction–exhumation process in the Upper sequence and all rocks have been strongly deformed. The following description is based on the characteristics of the metamorphic rocks.

The Upper sequence consists of a thick, monotonous pile of mica schists alternating with minor lenses of amphibolites, graphite schists, metacherts, calc-silicate lenses, greywackes and quartzites (Fig. 2b). A

Fig. 2. Idealized stratigraphic columns summarizing the main sedimentological features observed in the Lower (a) and Upper (b) sequences. The position of the analyzed samples is shown.

layer of amphibolites tens of meters thick occurs at the base of the sequence in the Malpica-Tui Unit, although the tectonic and subtractive character of the contact, marked by an ultramilonite mainly developed on rocks of the Lower sequence (ortho- and paragneisses), hides the true basal part of the Upper sequence. The amphibolites represent N-MORB basalts (Rodríguez, 2005) and also occur throughout the sequence, but are only abundant and of significant size in the lower levels. The decrease in amphibolitic rocks toward the top of the sequence coincides with an increase in graphite-bearing schists and metacherts. At the same time, the thickness and abundance of albite-bearing paragneisses representing the more arenaceous facies decrease rapidly towards the top.

2.3. Significance of the sedimentary record

The sedimentary record of both sequences has been heavily deformed and partly obliterated by Variscan subduction and collision, but their stratigraphic and petrologic characteristics permit a general overview of the outermost part of the northern margin of Gondwana. The fact that the preserved record may represent only a small part of a much thicker sequence cannot be ruled out, but the monotonous character of the two sequences is assumed to be representative of the entire record.

Qualitative comparison of the two sequences shows fundamental differences between them.

The Upper sequence represents a dominantly pelitic deposit with minor arenaceous levels at the base, progressive enrichment in organic material towards the top, and an important influx of basaltic material synchronous with sedimentation.

The Lower sequence is dominantly a greywacke deposit, several thousand meters thick, with scattered pelitic and graphitic levels. No volcanic rocks have been identified, but intrusive rocks postdating sedimentation are abundant, and include calc-alkaline granitoids and a bimodal alkaline suite that includes peralkaline units.

These differences in the stratigraphic record permit these sequences to be broadly placed in different paleogeographic settings.

The sediments of the Lower sequence were deposited close to the source area, probably in an active geodynamic setting that provided large amounts of detrital material derived from the erosion of relief created by tectonic activity. A strongly subsiding basin adjacent to this topographic relief is inferred to have accommodated the detrital supply. The sedimentological features point to a turbiditic setting, with the thick greywacke layers representing pulses of tectonic activity. The quartzites close to the top of the record may represent the transition to a continental platform on the coastal side of the basin once the major tectonic activity in the source area declined.

On the other hand, the sediments of the Upper sequence represent a distal, deeper depositional regime, still connected to an active setting that provided the volcanic (and probably the arenaceous material) during episodes of activity. The enrichment in organic material and presence of cherts, and the upward decrease in the arenaceous content, point to a progressive widening of the basin and/or its progressive separation of the main source area.

In both sequences, calc-silicate lenses represent carbonate-rich protoliths that can be compared with limestones occurring in the Neoproterozoic, early Cambrian, Late Ordovician, Silurian and Devonian of the Iberian autochthon (Díez Balda, 1986; Pérez-Estaún et al., 1990; Martínez Catalán et al., 2004a). But, as no significant limestone levels have been found in the allochthonous sequences, these cannot be used for correlation with the shallower deposits of the Gondwanan continental platform.

3. Sample description

Eight samples of the most representative lithologies were collected (Fig. 1b), five in the Lower sequence (BA-4, BA-5, BA-6, BA-7 and BA-8) and three in the Upper sequence (BA-1, BA-9 and BA-12). Their position in the stratigraphic columns is shown in Fig. 2.

Samples B4 to B8 are representative of the Lower sequence. BA-4, 5 and 6 are greywackes from the lower part of the sequence, BA-5 representing a more deformed and metamorphosed greywacke than the massive BA-4 and BA-6. Sample BA-7 corresponds to the quartzites in the upper part of the sequence, and BA-8 represents the more pelitic facies in the Lower sequence.

BA-4 is a mildly deformed metagreywacke sampled from a massive layer 40 cm thick, in which irregular clasts of feldspar, quartz and mica are surrounded by a partly recrystallized pelitic matrix. Small albite porphyroblasts include tiny crystals of garnet, white mica and chlorite, although their metamorphic growth does not disturb the massive internal structure of the sandstone. The detrital grains show undulose extinction. Their relationship to the Variscan deformation cannot be clearly established but assumed.

Sample BA-5 is an albite-bearing paragneiss with a crenulation cleavage folding a previous amphibolite facies fabric that represents the main foliation. The latter is related to exhumation during Variscan collision following early Variscan subduction (Martínez Catalán et al., 1996; Llana-Fúnez, 2001; Rodríguez, 2005). The paragneiss is composed of the stable assemblage quartz + white mica + biotite + albite ± garnet ± ilmenite. Albite porphyroblasts include an internal schistosity defined by quartz + phengite + garnet ± rutile ± epidote, which represents a high-pressure, medium temperature assemblage that records the initial subduction event (Gil Ibarguchi and Ortega Gironés, 1985). The main foliation is bent by microfolds with vertical axial planes and gently plunging axes associated with the development of a late crenulation cleavage defined by the reorientation of the plagioclase, biotite, quartz, and white mica of the main foliation, and the growth of new biotite, white mica, and quartz defining a tectonic banding.

BA-6 is a massive metagreywacke transformed into an albite-bearing paragneiss with a poorly developed planar foliation defined by quartz, biotite, and white mica. The main foliation is oblique to the compositional layering, which can be recognized at the layer boundary where the sample was collected. The albite porphyroblasts also include the same high-pressure assemblage described in BA-5.

BA-7 is a fine-grained quartzite with small amounts of white mica. The main foliation is formed by the statistical orientation of quartz grains, micas and minor quantities of opaque minerals. Quartz grains show internal deformation features, but the white mica does not define a true tectonic banding. The sample was collected from a homogeneous layer surrounded by mica-rich quartzites.

BA-8 is an albite-bearing mica schist with a foliation typical of the chlorite–biotite zone, composed of chlorite + quartz + albite + white mica ± biotite ± opaque minerals. The albite porphyroblasts include an internal fabric with folded patterns strongly oblique to the external foliation. The latter is formed by phengite, chlorite, quartz, rutile and rare garnet, and is comparable to the high-pressure internal foliation described in other samples (see BA-5).

The samples from the Upper sequence are pelitic rocks (BA-1 and BA-12) that occasionally include more arenaceous horizons (BA-9). The three samples are garnet-bearing mica schists with a main foliation whose stable mineral assemblage varies. For BA-1, the foliation is defined by garnet + white mica + biotite + albite + quartz ± illmenite, whereas in BA-9 and BA-12, it consists of garnet + quartz + white mica + albite + chloritoid + epidote ± rutile. In all of the samples the albite porphyroblasts contain an internal fabric defined by garnet + phengite + rutile + quartz ± glaucophane, which is also preserved as helicitic or straight inclusions in porphyroblastic garnet (BA-9 and BA-12) and chloritoid (BA-9). C′ extensional shear bands composed of quartz + white mica + chlorite crosscut and retrograde the main foliation in all samples. The main foliation in each sample represents a different stage of exhumation from blueschist facies (preserved in the internal fabric) to greenschist facies conditions (extensional shear

bands). A more detailed petrographic description can be found in Arenas et al. (1995), Rodríguez (2005) and López Carmona et al. (2008a,b, 2010).

4. Analytical methodology: U–Pb zircon dating

Zircon was recovered by the usual procedure of separation of heavy minerals: crushing, sieving and concentration of the heavy fraction using a Wilfley table, followed by magnetic and density separation. The final mineral fractions were hand-picked under a binocular microscope, mounted in Epoxy resin, and polished to an equatorial section of the grains.

All samples contain subidiomorphic zircons with rounded rims and variable shape and size. Their colour varies from clear and colourless to pinkish and almost opaque. The poorest sorting and less rounded shapes are in the greywackes, whereas grains from the mica schists and quartzites are more homogeneous, of smaller size (smaller for the mica schists) and more rounded shapes.

Prior to the analysis, the internal structure, inclusions, fractures and physical defects were identified using cathodoluminiscence imagery (CL). Characterizing the internal structure allows layers of zircon that grew during different events to be identified and linked to different processes. The CL study shows that most of the zircons have a similar core-rim internal texture. The cores usually exhibit concentric oscillatory zoning, typical of zircon grains crystallized in granitic magmas (Hoskin, 2000). Small metamorphic rims were detected in a few grains, but they were always too small to be analyzed. Only the more homogeneous part of the grain cores, free of defects, cracks and inclusions were analyzed. Some grains exhibit multiple and concentric layers of growth. No significant variation in the age of crystallization along each analyzed grain was detected.

4.1. LA-ICP-MS U–Pb dating

Uranium and lead isotopes were analyzed using a ThermoScientific Element 2 sector field ICP-MS coupled to a New Wave Research UP-213 ultraviolet laser system at Goethe-University Frankfurt following the method described by Gerdes and Zeh (2006, 2009).

Data were acquired in time resolved-peak jumping-pulse counting mode over 670 mass scans during a 19 s background measurement followed by a 25 s sample ablation. Laser spot-sizes varied from 30 to 40 μm with a typical penetration depth of ~15–20 μm. Signal was tuned to maximum sensitivity for Pb and U while keeping oxide production, monitored as $^{254}UO/^{238}U$, well below 1%. A teardrop-shaped, low volume (<2.5 cm^3) laser cell with a fast response (<1 s) and low wash-out time was used (Janoušek et al., 2006; Frei and Gerdes, 2009). With a depth penetration of ~0.6 μm s^{-1} and a 0.9 s integration time (=15 mass scans = 1 ratio) any significant variation of the Pb/Pb and U/Pb in the micrometer scale is detectable.

Raw data were corrected offline for background signal, common Pb, laser-induced elemental fractionation, instrumental mass discrimination, and time-dependent elemental fractionation of Pb/U using an in-house MS Excel® spreadsheet program (Gerdes and Zeh, 2006, 2009). A common Pb correction based on the interference-and background-corrected ^{204}Pb signal and a model Pb composition (Stacey and Kramers, 1975) was carried out, where necessary. The necessity of the correction was based on whether or not the corrected $^{207}Pb/^{206}Pb$ lay outside the internal errors of the measured ratios. This was the case for less than 10% of the analyses.

Uncertainties related to the common Pb correction (e.g. 4% uncertainty on the assumed $^{207}Pb/^{206}Pb$ composition) were quadratically added to final uncertainty. The interference of ^{204}Hg (mean = 129 ± 18 cps; counts per second) on the mass 204 was estimated using a $^{204}Hg/^{202}Hg$ ratio of 0.2299 and the measured ^{202}Hg. Laser-induced elemental fractionation and instrumental mass discrimination were corrected by normalization to the reference zircon GJ-1 (Jackson et al., 2004). Prior to this normalization, the drift in inter-elemental fractionation (Pb/U) during 30 s sample ablation was corrected for the individual analysis.

The correction was done by applying a linear regression through all measured ratios, excluding the outliers (±2 standard deviation; 2SD), and using the intercept with the *y*-axis as the initial ratio. The total offset of the measured drift-corrected $^{206}Pb/^{238}U$ ratio from the "true" IDTIMS value of the analyzed GJ-1 grain was typically around 3–9%. Reported uncertainties (2σ) of $^{206}Pb/^{238}U$ were propagated by the quadratic addition of the external reproducibility (2SD) obtained from the standard zircon GJ-1 ($n = 12$; 2 SD ~1.3%) during the analytical sequence (55 unknowns plus 12 GJ-1) and the within-run precision of each analysis (2 SE; standard error).

The external reproducibility of the $^{207}Pb/^{206}Pb$ of GJ-1 was about 0.9% (2 SD). However, as $^{207}Pb/^{206}Pb$ uncertainty during LA-SF-ICP-MS analysis is directly dependent on ^{207}Pb signal strength, uncertainties were propagated following Gerdes and Zeh (2009). The ^{235}U was calculated from the ^{238}U divided by 137.88 and the $^{207}Pb/^{235}U$ uncertainty by the quadratic addition of the $^{206}Pb/^{238}U$ and the $^{207}Pb/^{206}Pb$ uncertainty.

5. Age spectra

Only concordant or nearly concordant (<10% discordant) data were considered for interpretation of detrital zircon age. Fig. 3 includes all the U–Pb concordia diagrams showing the results of LA-ICP-MS dating with 2σ errors for the ellipses. The enlarged regions show the Paleozoic and Neoproterozoic zircons. Ratios and ages (in bold) for the selected analyses are given in Tables 1–8 (supplementary item in data repository). Ages younger than 1 Ga are reported based on $^{206}Pb/^{238}U$ ratios corrected for common Pb. Older ages are reported based on their ^{204}Pb-corrected $^{206}Pb/^{207}Pb$ isotopic ratio. Figs. 4 and 5 include all the probability and frequency diagrams made for each sample. As the samples belonging to each sedimentary sequence do not show significant differences, they have been integrated in single diagrams plotted for each representative lithology (plots with a light-grey background).

5.1. The greywackes of the Lower sequence

Samples BA-4, BA-5, BA-6 and BA-8 represent the greywackes of the Lower sequence and have been plotted in Fig. 4a, b, c, and d. The main group of zircons has Neoproterozoic $^{206}Pb/^{238}U$ ages between 540 and 750 Ma, with the maximum density around 650 Ma. The second group includes Paleoproterozic $^{207}Pb/^{206}Pb$ ages ranging between 1850 and 2250 Ma. Three relative maxima can be identified in this group. The first is around 1950 Ma, the second at 2050 Ma, and the third around 2150–2200 Ma. A widespread population of analyses with Archean ages represents the third group. It ranges between 2500 and 3500 Ma with two relative maxima at 2700 and 2850 Ma. A few clusters of Mesoproterozoic zircons also occur. Their ages form part of a continuous interval from 750 Ma (Neoproterozoic) to 1250 Ma, with several analyses around 1500 and 1600 Ma, but with a maximum abundance located between 800 and 1100 Ma.

The youngest zircon found yielded an age of 537 ± 17 Ma (98% concordance) and the youngest population age is 566 Ma old. The oldest zircon yielded an age of 3522 ± 11 Ma (101% concordance).

5.2. The quartzites of the Lower sequence

Sample BA-7 represents the quartzites of the Lower sequence and has been plotted in Fig. 4e. The main group is represented by 70 analyses with Neoproterozoic $^{206}Pb/^{238}U$ ages ranging between 551 and 993 Ma, with the maximum density around 650 Ma. The second group includes 58 analyses with Paleoproterozoic $^{207}Pb/^{206}Pb$ ages ranging between 1650 and 2450 Ma. Three main sub-maxima can be identified in this group. The first is around 1930 Ma, the second

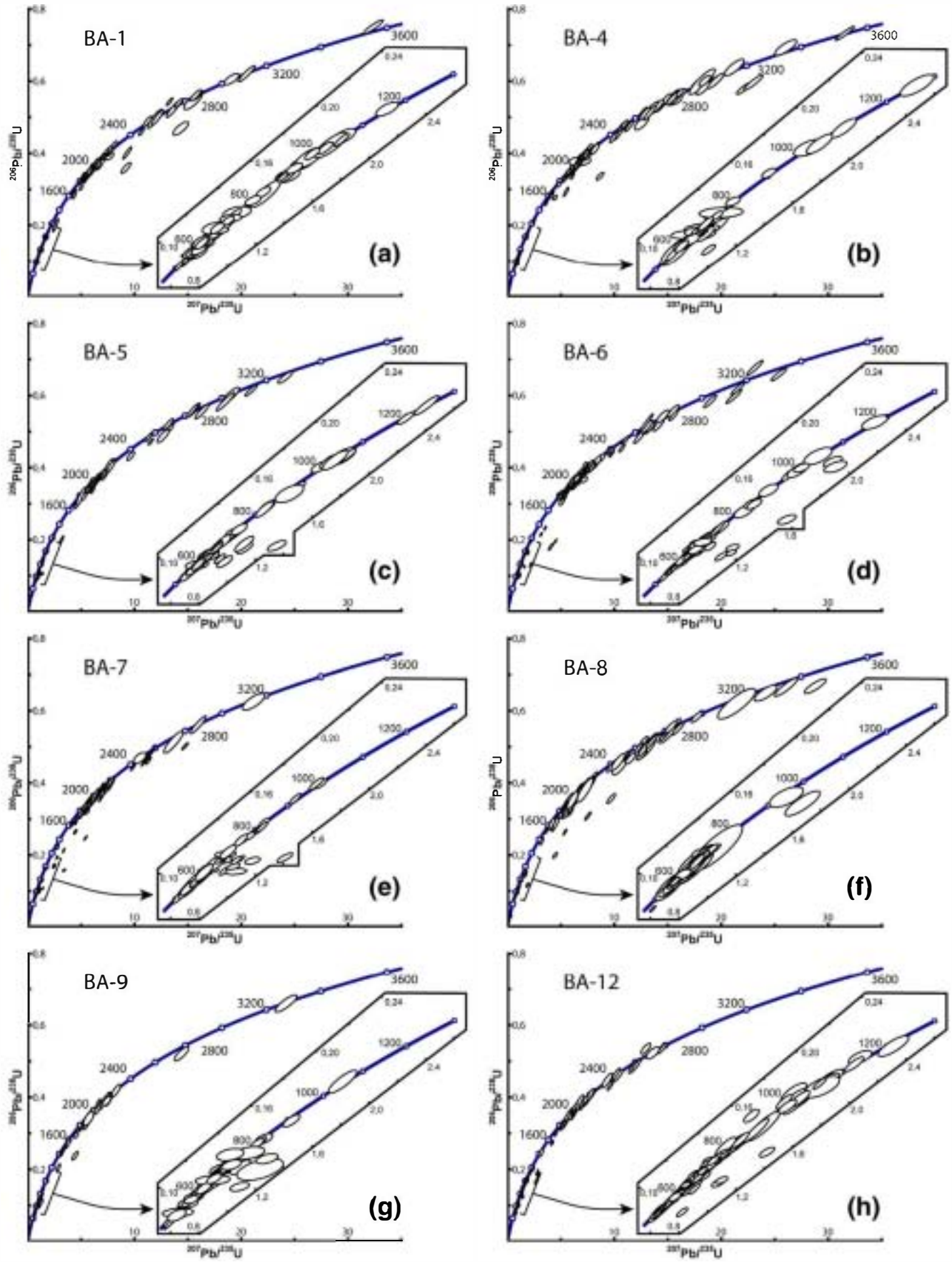

Fig. 3. U–Pb concordia diagrams showing the results of LA-ICP-MS dating of detrital zircons for all the samples. Error ellipses represent 2σ uncertainties. Phanerozoic and Neoproterozoic ages have been enlarged for clarity.

between 2000 and 2050 Ma, and the third between 2150 and 2200 Ma. Only a few irregularly distributed clusters of Mesoproterozoic and Archean ages occur. The Neo- to Mesoproterozoic input straddles the interval between 750 and 1000 Ma.

The youngest zircon is 551 ± 53 Ma old (108% concordance) and the youngest population age is 557 Ma. The oldest zircon yielded an age of 3137 ± 43 Ma (101% concordance).

5.3. The sediments of the Upper sequence

Probability and frequency diagrams of samples BA-1, BA-9 and BA-12 appear in Fig. 5a, b, and c, and all ages have been plotted together in Fig. 5d. The main group of zircons is represented by the analyses with Neoproterozoic $^{206}Pb/^{238}U$ ages between 500 and 750 Ma, with the maximum density around 650 Ma. The second group includes analyses with Paleoproterozic $^{207}Pb/^{206}Pb$ ages between 1850 and 2200 Ma. Three different relative maxima can be identified in this group: 1950 Ma, 2050 Ma, and 2150–2200 Ma. A widespread population of analyses with Archean ages ranging between 2500 and 3500 represents the third group. A few clusters of Neo- to Mesoproterozoic zircons occur that complete a continuous interval from 800 Ma (Neoproterozoic) to 1250 Ma. The maximum input ranges between 900 and 1050 Ma. A few analyses around 1400 and 1600 Ma also occur.

The youngest zircon has an age of 497 ± 22 Ma (93% concordance) and the youngest population age is 512 Ma. The oldest zircon is 3537 ± 14 Ma old (102% concordance).

6. Data integration and geological implications

6.1. Ages and geodynamic setting

The zircon age populations of the Basal allochthonous units studied here can be easily correlated with those of the autochthonous sequences of NW Iberia published by Fernández-Suárez et al. (2002a,b), Gutiérrez-Alonso et al. (2003), and Martínez Catalán et al. (2004b, 2008), which suggests that the Basal units are only moderately allochthonous, representing far-travelled domains but not exotic terranes. Our data support the idea that the Basal allochthonous units remained attached to the northern margin of Gondwana during the opening of the Rheic Ocean. This would explain why their subduction that occurred in the Late Devonian was the first Variscan deformation to affect this part of the outermost margin of Gondwana.

Our study also places tight constraints on the age of sedimentation. Given the statistical uncertainty of a single analysis, the youngest zircon population would represent a good approximation of the maximum age of sedimentation. Since the Lower sequence is intruded by late Cambrian calc-alkaline granitoids (ca. 495 Ma; Abati et al., 2010), and its youngest detrital zircon population is 566 Ma for the greywackes and 557 Ma for the quartzites, deposition is bracketed between the Neoproterozoic and the middle Cambrian. The Lower sequence represents deposition in a tectonically active setting, so the youngest population likely represents a good approximation of the age of sedimentation. Given the high content of Paleoproterozoic and Archean ages in all the samples from the Lower sequence (Fig. 4e and f), we suggest that the quartzites and metagreywackes were derived from a more cratonic source than the sediments of the Upper sequence. This input likely reflects not only the cratonic influence of a passive margin, but also the denudation of an arc built upon an old continental crust.

650 Ma is a common maximum for zircon age populations in sediments related to the Avalonian–Cadomian active margin along northern Gondwana. This maximum occurs in sediments that range in age from 545 to 570 Ma (Linnemann et al., 2004), which is consistent with the age proposed for the greywackes. Accordingly, we propose a late Neoproterozoic age for the sediments of the Lower sequence. They were probably laid down during the late pulses of the Avalonian–Cadomian arc-system, either in a back arc or retroarc setting (Murphy and Nance, 1991; Fernández-Suárez et al., 2000; Murphy et al., 2002; Pereira et al., 2006; Linnemann et al., 2007, 2008). In this scenario, the quartzites could represent the passive margin on the Gondwanan side of the arc (Fig. 6a).

The Upper sequence represents deposition that either pre-dates or is caused by the opening of the Rheic Ocean, as constrained by ca. 497 Ma granitoids intruded into the back-arc related ophiolite of Vila de Cruces (Arenas et al., 2007). The age of the youngest population (512 Ma) and the youngest zircons (around 500 Ma) in the Upper sequence coincide with one of the two main magmatic episodes registered in the Basal and Upper allochthonous units. The abundance of middle to late Cambrian ages in this sequence (Fig. 5d) suggests a direct linkage with the arc-related event, rather than the rift-related event dated as Early Ordovician (Rodríguez et al., 2007).

There is also a significant population of Avalonian–Cadomian zircons in the Upper sequence, which is the main population in the late Neoproterozoic greywackes of the Lower sequence. Erosion of the Cadomian arc-system would supply the same age population in both the Ediacaran and early Paleozoic. However, recycling of the Cadomian basement can also be envisaged, since Cambro-Ordovician magmatism is widespread in the Iberian autochthon and the Lower sequence of the Basal allochthonous units (Valverde-Vaquero and Dunning, 2000; Bea et al., 2006; Montero et al., 2007; Díez Montes et al., 2010).

The volcanic input in the Upper sequence can be placed into an extensional context, in which N-MORB basalts would have been incorporated during back-arc spreading (Fig. 6b). This interpretation is consistent with the sedimentological record, since the volcanic rocks were emplaced at the time of basin development and widening. This setting is considered to represent the first stage in the evolution of the Rheic Ocean by Sánchez Martínez (2009).

At the same time, flyschoid deposits with a large input of Cambrian zircons were accumulating close to the drifting arc (Fernández-Suárez et al., 2003; Fuenlabrada et al., 2010). These sediments are preserved in the Upper allochthonous units of the European Variscides, and may have been located along the more active side of the back-arc basin, attached to the arc-system. We consider them to be the proximal facies of the Cambrian arc, whereas the Upper sequence of the Basal allochthonous units represents contemporaneous distal deposits along the Gondwanan side of the basin during the middle to late Cambrian (Fig. 5b). Even if they are related to an active Cambrian setting, the flyschoid deposits of the Upper allochthonous units still include a remarkable number of cratonic Paleoproterozoic and Archean ages, as well as the Avalonian–Cadomian signature, which points to the ensialic character of the arc.

6.2. Paleogeographic constraints

No significant differences in cratonic input have been found in the sequences of the two tectonic units. They show the same dominant age populations and even the same minor peaks in the Paleoproterozoic input, although the latter are more pronounced in the older sediments of the Lower sequence. Furthermore, no differences appear to exist between the age populations of the two units and those of the NW Iberian autochthon. However, the relative proportions of early Neoproterozoic and late Mesoproterozoic zircons (corresponding to the 750–1150 Ma interval) are different. Whereas in the Basal units they represent 2–8% of the concordant analyses (Figs. 4 and 5), in late Ordovician, early Silurian and early Devonian quartzites of the autochthon, they amount to 24–38% (Martínez Catalán et al., 2004b). Similar abundances also occur in early Ordovician quartzites and greywackes, early Cambrian quartzites and late Neoprotezocoic sandstones (Fernández-Suárez et al., 2000, 2002a; Gutiérrez-Alonso et al., 2003).

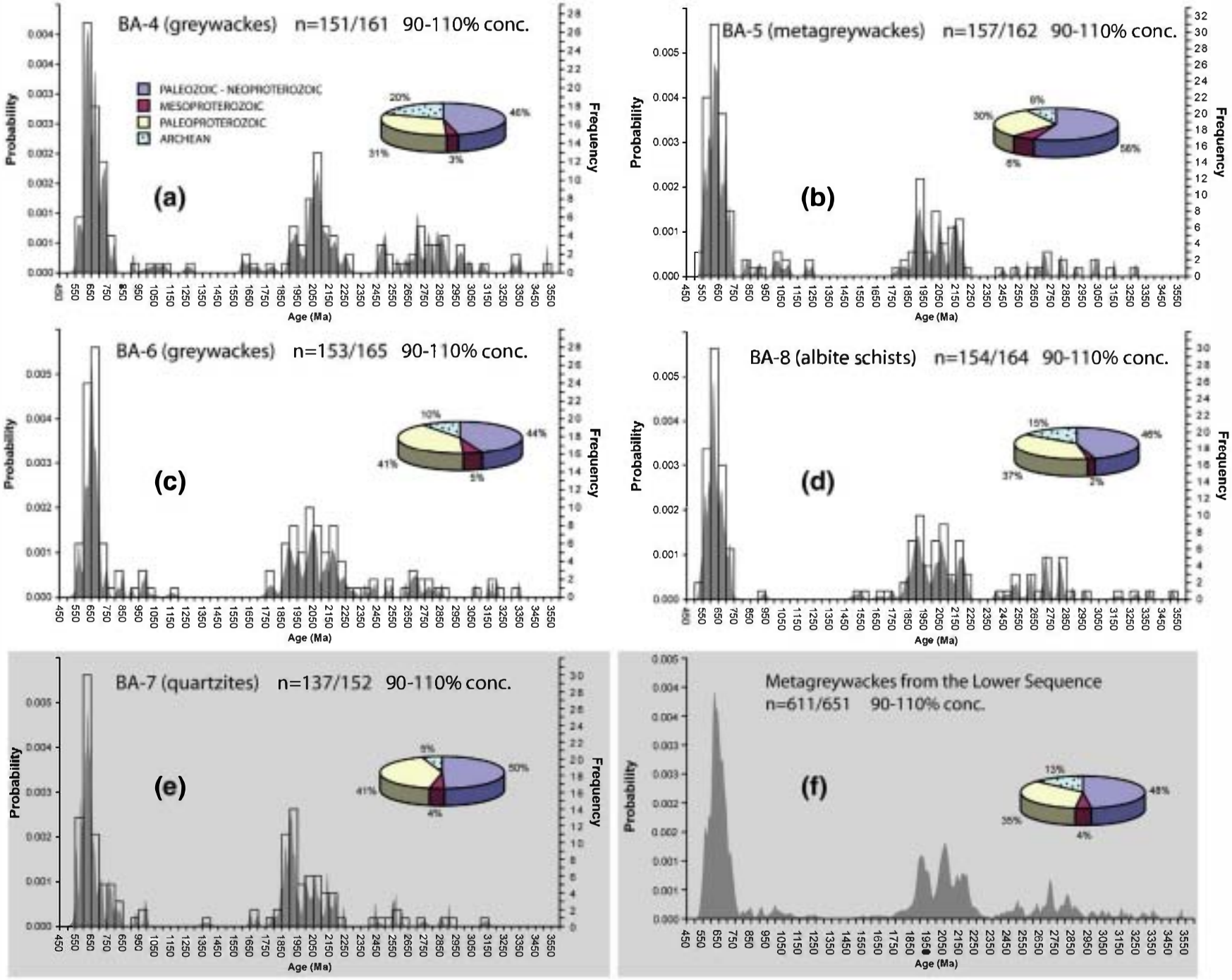
BA-4 (greywackes) n=151/161 90-110% conc.
PALEOZOIC - NEOPROTEROZOIC
MESOPROTEROZOIC
PALEOPROTEROZOIC
ARCHEAN
20%
46%
31%
3%
(a)
BA-5 (metagreywackes) n=157/162 90-110% conc.
6%
30%
56%
8%
(b)
BA-6 (greywackes) n=153/165 90-110% conc.
10%
44%
41%
5%
(c)
BA-8 (albite schists) n=154/164 90-110% conc.
15%
46%
37%
2%
(d)
BA-7 (quartzites) n=137/152 90-110% conc.
9%
50%
41%
4%
(e)
Metagreywackes from the Lower Sequence
n=611/651 90-110% conc.
13%
48%
35%
4%
(f)
Probability
Frequency
Age (Ma)

Neoproterozoic, Paleoproterozoic and Archean ages in both the Basal allochthonous units and the NW Iberian autochthon strongly suggest a West African craton provenance for most of the zircons (Nance and Murphy, 1994). But the middle Neoproterozoic to Mesoproterozoic signature (750–1150 Ma) is absent in the West African craton (Rocci et al., 1991; Boher et al., 1992; Potrel et al., 1998; Hirdes and Davis, 2002; Gueye et al., 2007). The two closer source areas identified to date for the Mesoproterozoic zircons are the couple formed by the Saharan craton and the Arabian–Nubian shield (Loizenbauer et al., 2001; Abdelsalam et al., 2002; Avigad et al., 2003, 2007; de Wit et al., 2005; Stern, 2008; Be'eri-Shlevin et al., 2009) in the eastern branch of the West African craton, and the Amazonian craton to the west (Bernasconi, 1987; Santos et al., 2000; Cordani and Teixeira, 2007).

The early Neoproterozoic (Tonian) and late Mesoproterozoic (Stenian; Walker and Geissman, 2009) record in the Basal units and the autochthon shows a continuous presence of zircon ages in the interval 750–1250 Ma (Figs. 3–5). The largest population occurs between 800 and 1100 Ma (Figs. 4e, f, and 5d), followed by a subordinate population between 1500 and 1650 Ma. Fig. 7 shows a simplified map of Gondwana at ca. 570 Ma with the main cratonic areas (and their characteristic isotopic ages) that may have acted as sources of detrital zircons for the northern Gondwana margin, according to Linnemann et al. (2007), and the main active zones during the late Neoproterozoic which could control the main detritus influx, including the Avalonian–Cadomian belt (Nance and Murphy, 1994) and the Trans-Brasiliano-Hoggar megasuture (Cordani and Teixeira, 2007).

Since NW Iberia cannot be placed far from either the West African craton or a Mesoproterozoic source, two possibilities arise for its paleoposition during the late Neoproterozoic to late Cambrian. The entire record of age populations roughly fits a paleoposition either between the eastern West African craton and the Saharan craton/Arabian–Nubian shield, or between West African craton and Amazonia (Friedl et al., 2000; Fernández-Suárez et al., 2002b; see also Melleton et al., 2010). Several arguments point to the first option, as discussed below.

Ages ranging 750–900 Ma, which represent most of the early Neoproterozoic zircons in our samples, are absent in the Amazonian craton, but exist along its eastern rim (Santos et al., 2000; Cordani and Teixeira, 2007), and also in the western rim of the Saharan craton (Abdelsalam et al., 2002 and references therein). These ages can be used as a guide to place the NW Iberian autochthon, because during that time interval, widespread magmatic and tectonic activities occurred in Amazonia (Pimentel et al., 1997; Cordani and Teixeira, 2007, and references therein) and Africa (Caby, 2003, and references therein), linked to the evolution of the Pampean–Goiás–Pharusian oceanic lithosphere (Cordani et al., 2003; Kröner and Cordani, 2003). This activity included extensive calc-alkaline magmatism corresponding to tectono-magmatic episodes of the Pan-African/Brasiliano orogenic cycle. The 750–900 Ma ages provide tight constrains on the paleoposition of sediments deposited in the northern margin of Gondwana, since the peri-Gondwanan and Pan-African/Brasiliano provenances strongly suggest a position between the West African and Saharan cratons (Fig. 7).

An overview of the timing and building processes in the Amazonian craton compiled by Cordani and Teixeira (2007) and Cordani et al. (2009) provides the age spectra that can be expected from its erosion and/or recycling. It includes, in the Rondonian–San Ignacio Province, an important source of zircons ranging 1300–1500 Ma, either derived from magmatic or metamorphic events. This interval is represented by extremely scarce zircon populations in our samples, which is difficult to explain if an Amazonian provenance is considered (Keppie et al., 2003) for the paleoposition of NW Iberia during the late Neoproterozoic, as suggested by Fernández-Suárez et al. (2002b) and Nance et al. (2008). Alternatively, potential African sources for the 1300–1500 Ma populations also exist in the Saharan craton (Abdelsalam et al., 2002).

Geochemistry of late Neoproterozoic siliciclastic rocks in an area of the NW Iberian autochthon suggests a homogeneous and recycled source, and favours a West Africa craton provenance (Ugidos et al., 2003a). Sm–Nd data from these sediments suggest a contribution of juvenile material, much younger than 1.1 Ga, and probably derived from pan-African orogens (650–700–900? Ma; Ugidos et al., 2003b).

Detrital micas from Cambrian sediments in the NW Iberian autochthon include the following populations: 550–640 Ma, c. 920–1060 Ma and 1580–1780 Ma (Gutiérrez-Alonso et al., 2005). The 550–640 Ma interval fits quite well in the Avalonian–Cadomian setting, whereas the two others fit both the African (Saharan) and Amazonian provenance. The presence of Mesoproterozoic detrital micas indicates the existence of rocks formed at that age that were eroded during the Cambrian. These ages, together with detrital zircon ages and geochemical data, have been interpreted as an evidence of a Mesoproterozoic basement occurring in the core of the Ibero-armorican arc (Gutiérrez-Alonso et al., 2005; Murphyet al., 2008). However, such interpretation is not supported by the inherited zircon ages of widespread Cambro-Ordovician granitoids and felsic volcanics intruded and erupted in the Iberian autochthon, Lower Allochthon and Basal units, where Mesoproterozoic ages are statistically meaningless. In fact, the zircon ages rather suggest a magmatic source mostly consisting of Neoproterozoic rocks (Valverde-Vaquero et al., 2005; Bea et al., 2007; Montero et al., 2007, 2009; Castiñeiras et al., 2008a,b; Díez Montes et al., 2010; Abati et al., 2010).

No late Neoproterozoic sutures or dextral mega-shear zones affecting the rim of northern Gondwana have been identified so far either in Iberia or the European Variscides. The models approximating Amazonia-derived terranes to northern African domains by along-strike movements rely only in the interpretation of Mesoproterozoic populations as derived from the Amazonian craton.

In short, we believe that the Mesoproterozoic ages interpreted as of Amazonian derivation in previous works are best explained by northern African sources in the light of new data in both South America and Africa (Santos et al., 2000; Loizenbauer et al., 2001; Abdelsalam et al., 2002; Avigad et al., 2003, 2007; de Wit et al., 2005; Cordani and Teixeira, 2007; Cordani et al., 2009; Ennih and Liégeois, 2008; Be'eri-Shlevin et al., 2009). The new sources support the building of the Cadomian belts by recycling of Paleoproterozoic basement, and provide a new role for the pan-African mobile zones involved in Gondwana assembly. For instance, the Trans-Brasiliano-Hoggar megasuture occurring along the eastern border of the West African and Amazonian cratons and the western border of the Saharan craton (Caby, 2003; Caby and Moiné, 2003; Ennih and Liégeois, 2008; Santos et al., 2008) could be the source of Neoproterozoic zircons ranging 900–530 Ma.

Assuming an African provenance, the relative proportions of Mesoproterozoic zircons in the two sequences analyzed, compared to those of the NW Iberian autochthon suggest that the Basal allochthonous units occupied a more western position, closer to the West African craton. Conversely, the Upper allochthonous units of NW Iberia are characterized by the absence of zircon age populations between the Ediacaran and the Paleoproterozoic (Fernández-Suárez et al., 2003), which suggests a more western derivation for this exotic terrane, the zircon ages record of which appears to have been derived almost exclusively from the West African craton (Fig. 7).

Fig. 4. Frequency (bars) and probability density distribution (curves) of ages, and relative abundance of significant age populations of detrital zircon grains of metagreywackes and quartzites from the Lower sequence. Plot (f), with a light-grey background, represents a cumulative diagram made by merging the data from all the greywackes of the Lower sequence. The quartzites (e) have also been shaded. Only concordant or subconcordant analyses (< 10% discordant) have been used for interpretation. *n*: number of analyses with < 10% discordance/total number of analyzed grains; conc.: concordance.

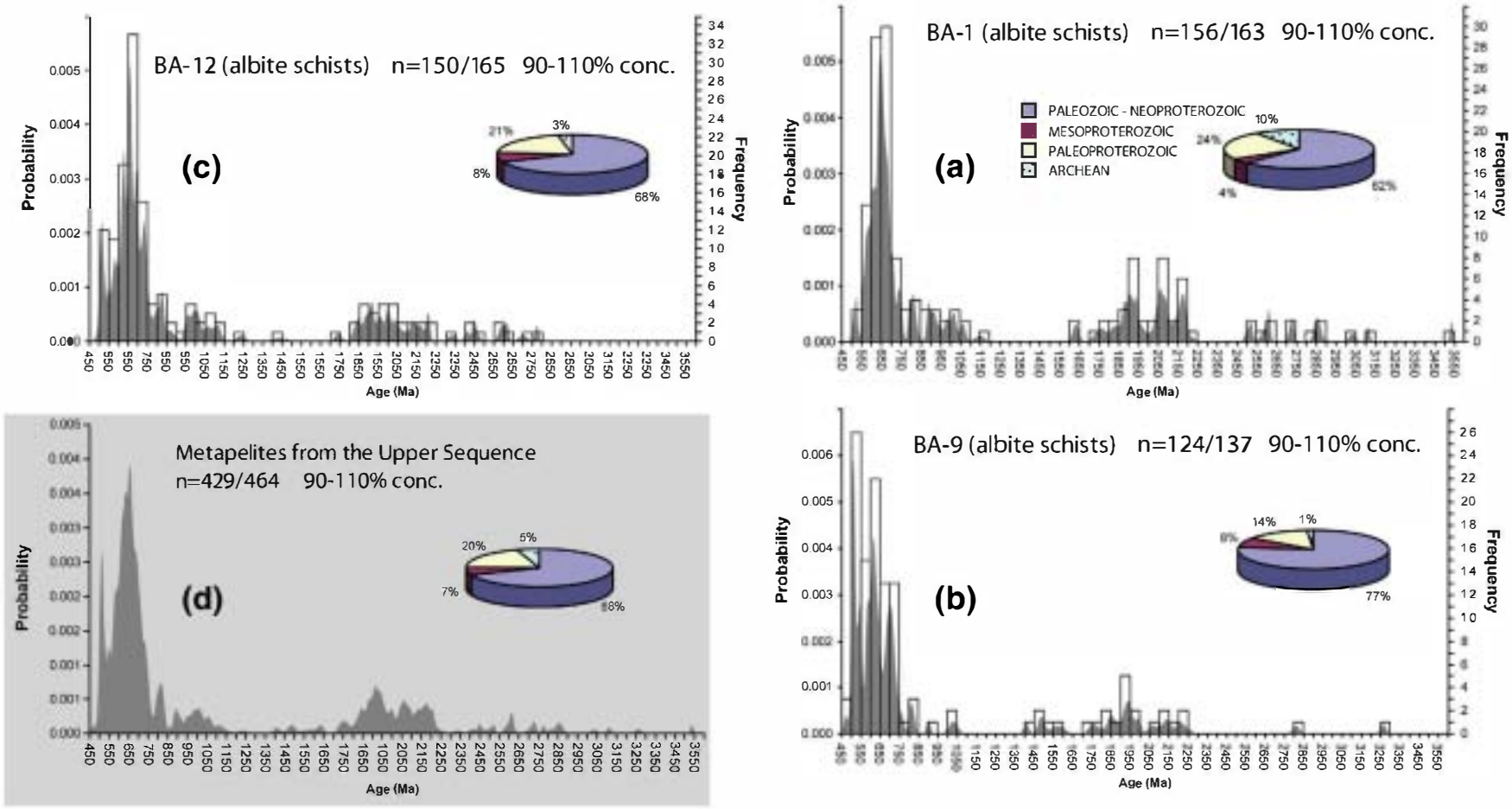

Fig. 5. Frequency (bars) and probability density distribution (curves) of ages, and relative abundance of significant age populations of detrital zircon grains of metapelites from the Upper sequence. Plot (d), with a light-grey background, represents a cumulative diagram made by merging the data from all the metapelites of the Upper sequence. Only concordant or subconcordant analyses (<10% discordant) have been used for interpretation. *n*: number of analyses with < 10% discordance/total number of analyzed grains; conc.: concordance.

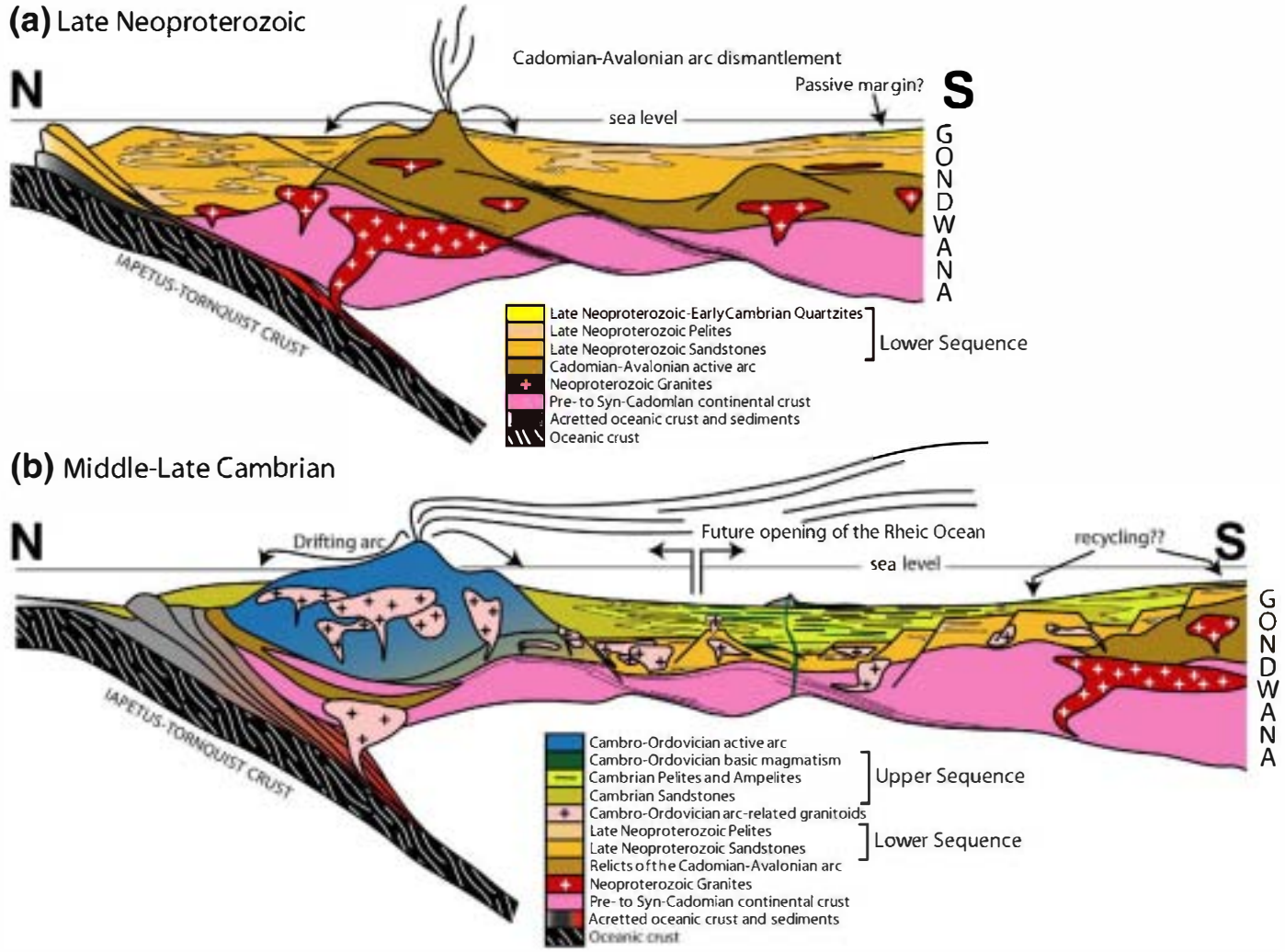

Fig. 6. Models for (a) the late Proterozoic and (b) middle-late Cambrian sedimentary sequences in the Iberian periphery of Gondwana. In (a), Neoproterozoic sediments in the Basal allochthonous units represent the last stages of Avalonian–Cadomian arc activity and its complete dismantlement in the outermost margin of the continent. Remnants of the magmatic suite related to the Neoproterozoic arc-system can be found covered by late Neoproterozoic and early Paleozoic sediments in the Iberian autochthon (Rodríguez Alonso et al., 2004). In (b), Cambrian sediments fill a back-arc basin related to drifting of a new ensialic arc. Cambro-Ordovician calc-alkaline magmatism intrudes the Neoproterozoic sediments, while roll-back of the oceanic slab forces the active arc to migrate oceanward, leaving behind synchronous deposits in the back arc and a tail of Cambro-Ordovician calc-alkaline intrusions. Recycling of the back-arc sediments and their Precambrian basement is expected during this process.

This model, first proposed by Gómez-Barreiro et al. (2007), does not require large-scale strike-slip movements during the late Precambrian and early Paleozoic as proposed by Fernández-Suárez et al. (2002b), because the South American source they proposed for the Mesoproterozoic zircons has been replaced by northern African sources, and the displacements necessary to join the Upper and Basal allochthonous units to NW Iberia can be explained by the widely reported dextral transcurrence between Laurrussia and Gondwana during the Devonian and Carboniferous (Gates et al., 1986; Rolet et al., 1994; Van Staal and De Roo, 1995; Franke and Zelazniewicz, 2002; Hatcher, 2002; Arenas et al., 2009). A dextral component of convergence has been considered responsible for the distribution of the different peri-Gondwanan terranes along the European Variscides (Shelley and Bossière, 2000, 2002; Stampfli et al., 2002; Martínez Catalán et al., 2007), and may have helped to join realms that were once in lateral continuity.

7. Conclusions

Two different metasedimentary sequences have been identified in the Basal Allochthonous units of NW Iberia. The sequences occur in thrust sheets whose boundaries were reworked during late Variscan extensional collapse, and have been mapped in the allochthonous complexes of Órdenes and Malpica-Tui. The Lower sequence is characterized by turbiditic facies, thick greywacke horizons, and relative proximity to the source area, probably the Neoproterozoic Avalonian–Cadomian arc. The Upper sequence is essentially pelitic with alternations of amphibolites with N-MORB affinity, and represents a more distal paleoenvironment in the back-arc basin of a Cambro-Ordovician volcanic arc.

Detrital zircons from five samples of the Lower sequence and three samples of the Upper sequence have yielded late Ediacaran and late Cambrian maximum depositional ages, respectively. The zircon age populations show no significant differences in the cratonic input of both sequences, although the cratonic influence is more pronounced in the Lower sequence. The age spectra are similar to published detrital zircon ages from the NW Iberian autochthon. This fact establishes the Basal allochthonous units as the outermost recognizable pieces of Gondwanan continental crust, and supports the idea that the early Paleozoic northern Gondwanan platform was extremely wide.

The zircon age populations of the Basal units have been used to locate the paleoposition of NW Iberia along the northern margin of Gondwana.

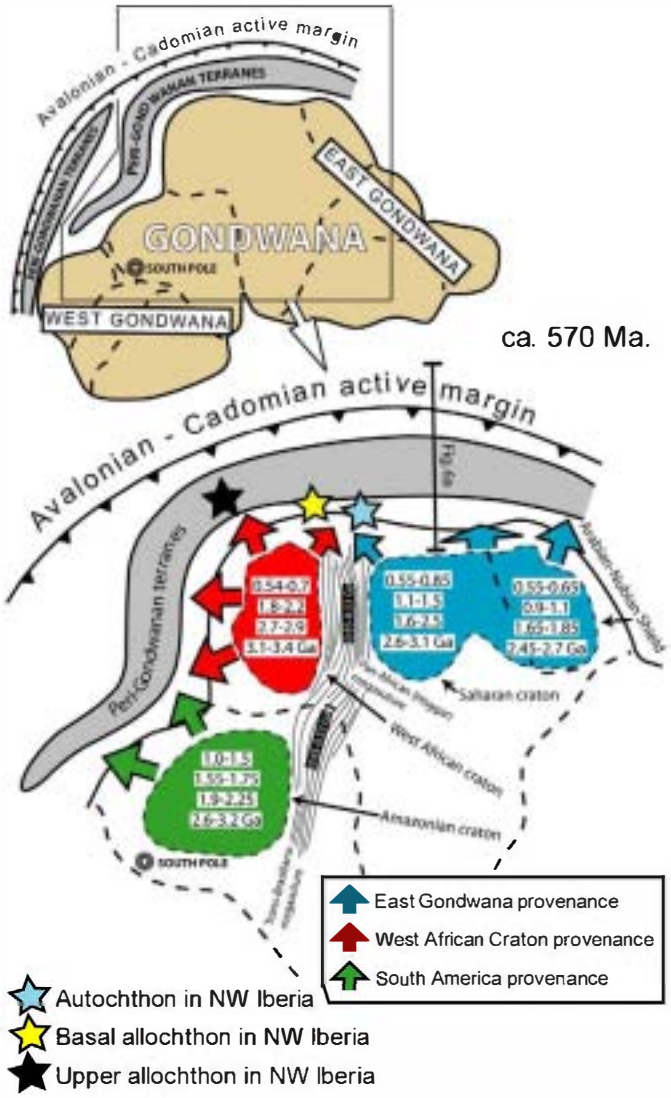

Fig. 7. Simplified paleogeography of Gondwana and related major peri-Gondwanan terranes at ca. 570 Ma (modified from Nance and Murphy, 1994; Cordani and Teixeira, 2007; Linnemann et al, 2007; Ennih and Liégeois, 2008; Cordani et al, 2009). The main source areas for the Avalonian–Cadomian active margin and Peri-Gondwanan terranes are highlighted and include cratons and the Trans-Brasiliano-Hoggar megasuture. The paleoposition of the NW Iberian autochthon is located between the West African craton and the Saharan craton, whereas the Basal allochthonous units were probably located closer to the West African craton. The upper allochthon in NW Iberia reflects a dominant West African craton provenance, so it has been placed further to the west. Numbers in the cratonic areas summarize their main age spectra for provenance constraints.

A position to the north of the West African craton is the most reasonable option, because (i) the sources of Mesoproterozoic ages are no longer exclusive of the Amazonian craton according with recent data, (ii) the tracers and implications derived for the Amazonian basement in NW Iberia are less clear than those for African, and (iii) the 750–900 Ma age population gives better constrains on tectonomagmatic processes affecting its eastern rim and the western rim of the Saharan craton than a South American source for the early Neoproterozoic zircons. This correlation does not require large-scale along-strike movements during the late Neoproterozoic to late Cambrian at the periphery of northern Gondwana, and gives a still poorly understood role to other pan-African sutures in the European Variscan terranes. A widely accepted dextral component of convergence between Laurussia and Gondwana during the closure of the Rheic Ocean may have joined realms that were once in lateral continuity and showed small differences in their provenance along the northern margin of Gondwana.

The sedimentological features of the two sequences described, their age, and the timing of magmatic events, have been integrated into a geodynamic model linked to the long-lived history of Neoproterozoic and Cambro-Ordovician subduction beneath northern Gondwana. The model involves an Avalonian–Cadomian active margin during the late Ediacaran, and a new arc that developed during the middle to late Cambrian with a back-arc basin between it and the newly formed passive margin of Gondwana. Sea floor spreading in the back arc gave birth to the Rheic Ocean around the Cambrian–Ordovician boundary.

Acknowledgments

This work has been funded by research projects CGL2007-65338-C02-01 and -02/BTE of the Dirección General de Programas y Transferencia del Conocimiento (Spanish Ministry of Science and Innovation). We are grateful to Damian Nance and Brendam Murphy for their helpful comments and suggestions, which in all cases improved the quality of the paper. Technicians from the Goethe Universität of Frankfurt am Main are also thanked.

Appendix A. Supplementary data

Supplementary data associated with this article can be found, in the online version, at doi:10.1016/j.gr.2009.12.006.

References

Abati, J., Dunning, G.R., Arenas, R., Díaz García, F., González Cuadra, P., Martínez Catalán, J.R., Andonaegui, P., 1999. Early Ordovician orogenic event in Galicia (NW Spain): evidence from U–Pb ages in the uppermost unit of the Ordenes Complex. Earth Planetary Science Letters 165, 213–228.

Abati, J., Arenas, R., Martínez Catalán, J.R., Díaz García, F., 2003. Anticlockwise P–T path of granulites from the Monte Castelo Gabbro (Órdenes Complex, NW Spain). Journal of Petrology 44, 305–327.

Abati, J., Gerdes, A., Fernández-Suárez, J., Arenas, R., Whitehouse, M.J., Díez Fernández, R., 2010. Magmatism and early-Variscan continental subduction in the northern Gondwana margin recorded in zircons from the basal units of Galicia, NW Spain. Geological Society of America Bulletin 122, 219–235. doi:10.1130/B26572.1.

Abdelsalam, M.G., Liégeois, J.P., Stern, R.J., 2002. The Saharan metacraton. Journal of African Earth Sciences 34, 119–136.

Andonaegui, P., González delTánago, J., Arenas, R., Abati, J., Martínez Catalán, J.R., Peinado, M., Díaz García, F., 2002. Tectonic setting of the Monte Castelo gabbro (Ordenes Complex, northwestern Iberian Massif): evidence for an arc-related terrane in the hanging wall to the Variscan suture. In: Martínez Catalán, J.R., Hatcher Jr. Jr., R.D., Arenas, R., Díaz García, F. (Eds.), Variscan–Appalachian Dynamics: The Building of the Late Paleozoic Basement, Geological Society of America Special Paper, vol. 364, pp. 37–56.

Arenas, R., Rubio Pascual, F.J., Díaz García, F., Martínez Catalán, J.R., 1995. High pressure micro-inclusions and development of an inverted metamorphic gradient in the Santiago Schists (Ordenes Complex, NW Iberian Massif, Spain): evidence of subduction and syn-collisional decompression. Journal of Metamorphic Geology 13, 141–164.

Arenas, R., Abati, J., Martínez Catalán, J.R., Díaz García, F., Rubio Pascual, F.J., 1997. P–T evolution of eclogites from the Agualada Unit (Ordenes Complex, NW Iberian Massif, Spain): implications for crustal subduction. Lithos 40, 221–242.

Arenas, R., Martínez Catalán, J.R., Sánchez Martínez, S., Fernández-Suárez, J., Andonaegui, P., Pearce, J.A., Corfu, F., 2007. The Vila de Cruces ophiolite: a remnant of the early Rheic Ocean in the Variscan suture of Galicia (NW Iberian Massif). Journal of Geology 115, 129–148.

Arenas, R., Sánchez Martínez, S., Castiñeiras, P., Jeffries, T.E., Díez Fernández, R., Andonaegui, P., 2009. The basal tectonic mélange of the Cabo Ortegal Complex (NW Iberian Massif): a key unit in the suture of Pangea. Journal of Iberian Geology 35, 85–125.

Avigad, D., Kolodner, K., McWilliams, M., Persing, H., Weissbrod, T., 2003. Origin of northern Gondwana Cambrian sandstone revealed by detrital zircon SHRIMP dating. Geology 31, 227–230.

Avigad, D., Stern, R.J., Beyth, M., Miller, N., McWilliams, M.O., 2007. Detrital zircon U–Pb geochronology of Cryogenian diamictites and lower Paleozoic sandstone in Ethiopia (Tigrai): age constraints on Neoproterozoic glaciation and crustal evolution of the southern Arabian–Nubian Shield. Precambrian Research 154, 88–106.

Be'eri-Shlevin, Y., Katzir, Y., Whitehouse, M.J., Kleinhanns, C., 2009. Contribution of pre Pan-African crust to formation of the Arabian Nubian Shield: new secondary ionization mass spectrometry U–Pb and O studies of zircon. Geology 37, 899–902.

Bea, F., Montero, P., Talavera, C., Zinger, T., 2006. A revised Ordovician age for the Miranda do Douro orthogneiss, Portugal. Zircon U–Pb ion-microprobe and LA-ICPMS dating. Geologica Acta 4, 395–401.

Bea, F., Montero, P., González-Lodeiro, F., Talavera, C., 2007. Zircon inheritance reveals exceptionally fast crustal magma generation processes in Central Iberia during the Cambro-Ordovician. Journal of Petrology 48, 2327–2339.

Bernasconi, A., 1987. The major Precambrian terranes of eastern South-America: a study of their regional and chronological evolution. Precambrian Research 37, 107–124.

Boher, M., Abouchami, W., Michard, A., Albarede, F., Arndt, N.T., 1992. Crustal growth in West Africa at 2.1 Ga. Journal of Geophysical Research 97, 345–369.

Caby, R., 2003. Terrane assembly and geodynamic evolution of central-western Hoggar: a synthesis. Journal of African Earth Sciences 37, 133–159.

Caby, R., Moiné, P., 2003. Neoproterozoic subductions and differential exhumation of western Hoggar (southwest Algeria): new structural, petrological and geochronological evidence. Journal of African Earth Sciences 37, 269–293.

Castiñeiras, P., Navidad, M., Liesa, M., Carreras, J., Casas, J.M., 2008a. U–Pb zircon ages (SHRIMP) for Cadomian and Early Ordovician magmatism in the Eastern Pyrenees: new insights into the pre-Variscan evolution of the northern Gondwana margin. Tectonophysics 461, 228–239.

Castiñeiras, P., Villaseca, C., Barbero, L., Martín Romera, C., 2008b. SHRIMP U–Pb zircon dating of anatexis in high-grade migmatite complexes of Central Spain: implications in the Hercynian evolution of Central Iberia. International Journal of Earth Sciences 97, 35–50.

Cordani, U.G., Teixeira, W., 2007. Proterozoic accretionary belts in the Amazonian Craton. In: Hatcher Jr. Jr., R.D., Carlson, M.P., McBride, J.H., Martínez Catalán, J.R. (Eds.), 4-D Framework of Continental Crust: Geological Society of America Memoir, vol. 200, pp. 297–320.

Cordani, U.G., D'Agrella-Filho, M.S., Brito-Neves, B.B., Trindade, R.I.F., 2003. Tearing up Rodinia: the Neoproterozoic paleogeography of South American cratonic fragments. Terra Nova 15, 350–359.

Cordani, U.G., Teixeira, W., D'Agrella-Filho, M.S., Trindade, R.I., 2009. The position of the Amazonian Craton in supercontinents. Gondwana Research 15, 396–407.

de Wit, M.J., Bowring, S., Dudas, F., Kamga, G., 2005. The great Neoproterozoic Central Saharan arc and the amalgamation of the North African Shield. GAC-MAC-CSPG-CSSS Joint Meeting, Halifax, Nova Scotia, Abstracts, vol. 30, pp. 42–43.

Díaz García, F., Arenas, R., Martínez Catalán, J.R., González del Tánago, J., Dunning, G., 1999. Tectonic evolution of the Careón ophiolite (Northwest Spain): a remnant of oceanic lithosphere in the Variscan belt. Journal of Geology 107, 587–605.

Díez Balda, M.A., 1986. El Complejo Esquisto-Grauváquico, las series paleozoicas y la estructura hercínica al Sur de Salamanca. Ph.D. thesis, Universidad de Salamanca.

Díez Fernández, R., Martínez Catalán, J.R., 2009. 3D analysis of an Ordovician igneous ensemble: a complex magmatic structure hidden in a polydeformed allochthonous Variscan unit. Journal of Structural Geology 31, 222–236.

Díez Montes, A., Martínez Catalán, J.R., Bellido Mulas, F., 2010. Role of the Ollo de Sapo massive felsic volcanism of NW Iberia in the Early Ordovician dynamics of northern Gondwana. Gondwana Research 17, 363–376.

Ennih, N., Liégeois, J.-P., 2008. The boundaries of the West African craton, with special reference to the basement of the Moroccan metacratonic Anti-Atlas belt. In: Ennih, N., Liégeois, J.-P. (Eds.), The boundaries of the West African craton: Geological Society of London Special Publication, vol. 297, pp. 1–17.

Fernández-Suárez, J., Gutiérrez-Alonso, G., Jenner, G.A., Tubrett, M.N., 2000. New ideas on the Proterozoic–Early Paleozoic evolution of NW Iberia: insights from U–Pb detrital zircon ages. Precambrian Research 102, 185–206.

Fernández-Suárez, J., Gutiérrez-Alonso, G., Cox, R., Jenner, G.A., 2002a. Assembly of the Armorica microplate: a strike-slip terrane delivery? Evidence from U–Pb ages of detrital zircons. Journal of Geology 110, 619–626.

Fernández-Suárez, J., Gutiérrez-Alonso, G., Jeffries, T.E., 2002b. The importance of along margin terrane transport in northern Gondwana: insights from detrital zircon parentage in Neoproterozoic rocks from Iberia and Brittany. Earth and Planetary Science Letters 204, 75–88.

Fernández-Suárez, J., Díaz García, F., Jeffries, T.E., Arenas, R., Abati, J., 2003. Constraints on the provenance of the uppermost allochthonous terrane of the NW Iberian Massif: inferences from detrital zircon U–Pb ages. Terra Nova 15, 138–144.

Floor, P., 1966. Petrology of an aegirine–riebeckite gneiss-bearing part of the Hesperian Massif: the Galiñeiro and surrounding areas, Vigo, Spain. Leidse Geologische Mededelingen 36, 1–204.

Franke, W., Zelazniewicz, A., 2002. Structure and evolution of the Bohemian arc. In: Winchester, J.A., Pharaoh, T.C., Verniers, J. (Eds.), Palaeozoic Amalgamation of Central Europe, London: Geological Society of London Special Publication, vol. 201, pp. 279–293.

Frei, D., Gerdes, A., 2009. Accurate and precise in-situ zircon U–Pb age dating with high spatial resolution and high sample throughput by automated LA-SF-ICP-MS. Chemical Geology 261, 261–270.

Friedl, G., Finger, F., Mcnaughton, N.J., Fletcher, I.R., 2000. Deducing the ancestry of terranes: SHRIMP evidence for South America-derived Gondwana fragments in central Europe. Geology 28, 1035–1038.

Fuenlabrada, J.M., Arenas, R., Sánchez Martínez, S., Díaz García, F., Castiñeiras, P., 2010. A peri-Gondwanan arc in NW Iberia I: Isotopic and geochemical constraints on the origin of the arc — A sedimentary approach. Gondwana Research 17, 338–351.

Gates, A.E., Simpson, C., Glover, L., 1986. Appalachian Carboniferous dextral strike-slip faults: an example from Brookneal, Virginia. Tectonics 5, 119–133.

Gerdes, A., Zeh, A., 2006. Combined U–Pb and Hf isotope IA-(MC)-ICP-MS analyses of detrital zircons: comparison with SHRIMP and new constraints for the provenance and age of an Armorican metasediment in Central Germany. Earth and Planetary Sciences Letters 249, 47–61.

Gerdes, A., Zeh, A., 2009. Zircon formation versus zircon alteration—new insights from combined U–Pb and Lu–Hf in-situ IA-ICP-MS analyses, and consequences for the interpretation of Archean zircon from the Central Zone of the Limpopo Belt. Chemical Geology 261, 230–243.

Gil Ibarguchi, J.I., Ortega Gironés, E., 1985. Petrology, structure and geotectonic implications of glaucophane-bearing eclogites and related rocks from the Malpica-Tuy (MT) Unit, Galicia, Northwest Spain. Chemical Geology 50, 145–162.

Gómez-Barreiro, J., Martínez Catalán, J.R., Díez Fernández, R., Arenas, R., Díaz García, F., (in review). Upper crust reworking during gravitational collapse: The Bembibre-Pico Sacro detachment system (NW Iberia).

Gómez-Barreiro, J., Martínez Catalán, J.R., Arenas, R., Castiñeiras, P., Abati, J., Díaz García, F., Wijbrans, J.R., 2007. Tectonic evolution of the upper allochthon of the Órdenes Complex (northwestern Iberian Massif): structural constraints to a polyorogenic peri-Gondwanan terrane. In: Linnemann, U., Nance, R.D., Kraft, P., Zulauf, G. (Eds.), The evolution of the Rheic Ocean: from Avalonian–Cadomian active margin to Alleghenian–Variscan collision: Geological Society of America Special Paper, vol. 423, pp. 315–332.

Gueye, M., Siegesmund, S., Wemmer, K., Pawlig, S., Drobe, M., Nolte, N., Layer, P., 2007. New evidences for an early Birimian evolution in the West African Craton: an example from the Kédougou–Kénieba inlier, southeast Senegal. South African Journal of Geology 110, 511–534.

Gutiérrez-Alonso, G., Fernández-Suárez, J., Jeffries, T.E., Jenner, G.A., Tubrett, M.N., Cox, R., Jackson, S.E., 2003. Terrane accretion and dispersal in the northern Gondwana margin. An Early Paleozoic analogue of a long-lived active margin. Tectonophysics 365, 221–232.

Gutiérrez-Alonso, G., Fernández-Suárez, J., Collins, A.S., Abad, I., Nieto, F., 2005. Amazonian Mesoproterozoic basement in the core of the Ibero-Armorican Arc: $^{40}Ar/^{39}Ar$ detrital mica ages complement the zircon's tale. Geology 33, 637–640.

Hatcher, R.D., 2002. Alleghanian (Appalachian) orogeny, a product of zipper tectonics: rotational, transpressive continent–continent collision and closing of ancient oceans along irregular margins. In: Martínez Catalán, J.R., Hatcher, R.D., Arenas, R., Díaz García, F. (Eds.), Variscan–Appalachian dynamics: the building of the Late Paleozoic basement, Boulder, Colorado: Geological Society of America Special Paper, vol. 364, pp. 199–208.

Hirdes, W., Davis, D.W., 2002. U–Pb geochronology of Paleoproterozoic rocks in the Southern part of the Kedougou-Kéniéba Inlier, Senegal, West Africa: evidence for diachronous accretionary development of the Eburnean Province. Precambrian Research 118, 83–99.

Hoskin, P.W.O., 2000. Patterns of chaos: fractal statistics and the oscillatory chemistry of zircon. Geochemica and Cosmochemica Acta 64, 1905–1923.

Jackson, S.E., Pearson, N.J., Griffin, W.L., Belousova, E.A., 2004. The application of laser ablation-inductively coupled plasma-mass spectrometry to in situ U–Pb zircon geochronology. Chemical Geology 211, 47–69.

Janoušek, V., Gerdes, A., Vrána, S., Finger, F., Erban, V., Friedl, G., Braithwaite, C.J.R., 2006. Low pressure granulites of the Lišov Massif, Southern Bohemia: Viséan metamorphism of late Devonian plutonic arc rocks. Journal of Petrology 47, 705–744.

Keppie, J.D., Nance, R.D., Murphy, J.B., Dostal, J., 2003. Tethyan, Mediterranean, and Pacific analogues for the Neoproterozoic–Paleozoic birth and development of peri-Gondwanan terranes and their transfer to Laurentia and Laurussia. Tectonophysics 365, 195–219.

Kröner, A., Cordani, U.G., 2003. African, southern Indian and South American cratons were not part of the Rodinia supercontinent: evidence from field relationships and geochronology. Tectonophysics 375, 325–352.

Linnemann, U., McNaughton, N.J., Romer, R.L., Gehmlich, M., Drost, K., Tonk, Ch., 2004. West African provenance for Saxo-Thuringia (Bohemian Massif): did Armorica ever leave pre-Pangean Gondwana?. U/Pb-SHRIMP zircon evidence and the Nd-isotopic record. International Journal of Earth Sciences 93, 683–705.

Linnemann, U., Gerdes, A., Drost, K., Buschmann, B., 2007. The continuum between Cadomian orogenesis and opening of the Rheic Ocean: constraints from LA-ICP-MS U–Pb zircon dating and analysis of plate-tectonic setting (Saxo-Thuringian zone, northeastern Bohemian Massif, Germany). Geological Society of America Special Paper 423, 61–96.

Linnemann, U., Pereira, F., Jeffries, T.E., Drost, K., Gerdes, A., 2008. The Cadomian Orogeny and the opening of the Rheic Ocean: the diacrony of geotectonic processes constrained by IA-ICP-MS U–Pb zircon dating (Ossa-Morena and Saxo-Thuringian Zones, Iberian and Bohemian Massifs). Tectonophysics 461, 21–43.

Llana-Fúnez, S., 2001. La estructura de la Unidad de Malpica-Tui (Cordillera Varisca en Iberia). IGME, Serie Tesis Doctorales 1, 1–295.

Loizenbauer, J., Wallbrecher, E., Fritz, H., Neumayr, P., Khudeir, A.A., Kloetzli, U., 2001. Structural geology, single zircon ages and fluid inclusion studies of the Meatiq metamorphic core complex: implications for Neoproterozoic tectonics in the Eastern Desert of Egypt. Precambrian Research 110, 357–383.

López Carmona, A., Abati, J., Reche, J., 2010. Petrologic modeling of chloritoid glaucophane schists from the NW Iberian Massif. Gondwana Research 17, 377–391.

López Carmona, A., Abati, J., Reche, J., 2008a. Evolución metamórfica de los esquistos de AP/BT de Ceán (Unidad de Malpica-Tui, NW del Macizo Ibérico). Geogaceta 43, 3–6.

López Carmona, A., Abati, J., Reche, J., 2008b. Phase equilibrium modelling in the KFMASH system to show the metamorphic evolution of the Ceán Schists (Malpica-Tui Unit, NW Iberian Massif). Geogaceta 44, 27–30.

Marquínez García, J.L., 1984. La geología del área esquistosa de Galicia Central (Cordillera Herciniana, NW de España). Memorias del Instituto Geológico y Minero de España 100, 1–231.

Martínez Catalán, J.R., Arenas, R., Díaz García, F., Rubio Pascual, F.J., Abati, J., Marquínez, J., 1996. Variscan exhumation of a subducted Paleozoic continental margin: the basal units of the Ordenes Complex, Galicia, NW Spain. Tectonics 15, 106–121.

Martínez Catalán, J.R., Arenas, R., Díaz García, F., Abati, J., 1997. Variscan acretionary complex of northwest Iberia: terrane correlation and succession oftectonothermal events. Geology 25, 1103–1106.

Martínez Catalán, J.R., Gutiérrez-Marco, J.C., Hacar, M.P., Barros Lorenzo, J.C., González Clavijo, E., González Lodeiro, F., 2004a. Zona Centroibérica: Estratigrafía, Secuencia preorogénica del Ordovícico-Devónico. In: Vera, J.A. (Ed.), Geología de España, SGE-IGME, pp. 72–75.

Martínez Catalán, J.R., Fernández-Suárez, J., Jenner, G.A., Belousova, E., Díez Montes, A., 2004b. Provenance constraints from detrital zircon U–Pb ages in the NW Iberian Massif: implications for Paleozoic plate configuration and Variscan evolution. Journal of the Geological Society 161, 461–473.

Martínez Catalán, J.R., Arenas, R., Díaz García, F., Gómez-Barreiro, J., González Cuadra, P., Abati, J., Castiñeiras, P., Fernández-Suárez, J., Sánchez Martínez, S., Andonaegui, P., Gónzalez Clavijo, E., Díez Montes, A., Rubio Pascual, F.J., Valle Aguado, B., 2007. Space and time in the tectonic evolution of the northwestern Iberian Massif. Implications for the Variscan belt. In: Hatcher Jr. Jr., R.D., Carlson, M.P., McBride, J.H., Martínez Catalán, J.R. (Eds.), 4-D Framework of Continental Crust: Geological Society of America Memoir, vol 200, pp. 403–423.

Martínez Catalán, J.R., Fernández-Suárez, J., Meireles, C., González-Clavijo, E., Belousova, E., Saeed, A., 2008. U–Pb detrital circón ages in synorogenic deposits of the NW Iberian Masif (Variscan Belt): interplay of Devonian–Carbonifeorus sedimentation and thrust tectonics. Journal of the Geological Society 165, 687–698.

Martínez Catalán, J.R., Arenas, R., Abati, J., Sánchez Martínez, S., Díaz García, F., Fernández-Suárez, J., González Cuadra, P., Castiñeiras, P., Gómez-Barreiro, J., Díez Montes, A., González Clavijo, E., Rubio Pascual, F.J., Andonaegui, P., Jeffries, T.E., Alcock, J.E., Díez Fernández, R., López Carmona, A., 2009. A rootless suture and the loss of the roots of a mountain chain: the Variscan belt of NW Iberia. Comptes Rendus Geoscience de l'Académie des sciences 341, 114–126.

Melleton, J., Cocherie, A., Faure, M., Rossi, P., 2010. Precambrian protoliths and Early Paleozoic magmatism in the French Massif Central: U–Pb data and the North Gondwana connection in the west European Variscan belt. Gondwana Research 17, 13–25.

Montero, P., Bea, F., González Lodeiro, F., Talavera, C., Whitehouse, M.J., 2007. Zircon ages of the metavolcanic rocks and metagranites of the Ollo de Sapo Domain in central Spain: implications for the Neoproterozoic to Early Palaeozoic evolution of Iberia. Geological Magazine 144, 963–976.

Montero, P., Talavera, C., Bea, F., González Lodeiro, F., Whitehouse, M.J., 2009. Zircon geochronology of the Ollo de Sapo Formation and the age of the Cambro-Ordovician rifting in Iberia. Journal of Geology 117, 174–191.

Murphy, J.B., Nance, R.D., 1991. Supercontinent model for the contrasting character of Late Proterozoic orogenic belts. Geology 19, 469–472.

Murphy, J.B., Eguiluz, L., Zulauf, G., 2002. Cadomian orogens, peri-Gondwanan correlatives and Laurentia–Baltica connections. Tectonophysics 352, 1–9.

Murphy, J.B., Gutiérrez-Alonso, G., Fernández-Suárez, J., Braid, J.A., 2008. Probing crustal and mantle lithosphere origin through Ordovician volcanic rocks along the Iberian passive margin of Gondwana. Tectonophysics 461, 166–180.

Nance, R.D., Murphy, J.B., 1994. Contrasting basement isotopic signatures and the palinspastic restoration of peripheral orogens: example from the Neoproterozoic Avalonian–Cadomian belt. Geology 22, 617–620.

Nance, R.D., Murphy, J.B., Strachan, R.A., Keppie, J.D., Gutiérrez-Alonso, G., Fernández-Suárez, J., Quesada, C., Linnemann, U., D'lemos, R., Pisarevsky, S.A., 2008. Neoproterozoic–early Palaeozoic tectonostratigraphy and palaeogeography of the peri-Gondwanan terranes: Amazonian v. West African connections. In: Ennih, N., Liegeois, J.-P. (Eds.), The Boundaries of the West African Craton, London: Geological Society of London Special Publication, vol 297, pp. 345–383.

Pereira, M.F., Chichorro, M., Linnemann, U., Eguiluz, L., Brandao Silva, J., 2006. Inherited arc signature in Ediacaran and Early Cambrian basins of the Ossa-Morena Zone (Iberian Massif, Portugal): paleogeographic link with European and North African Cadomian correlatives. Precambrian Research 144, 297–315.

Pérez-Estaún, A., Bastida, F., Martínez Catalán, J.R., Gutiérrez Marco, J.C., Marcos, A., Pulgar, J.A., 1990. West Asturian-Leonese Zone. Stratigraphy. In: Dallmeyer, R.D., Martínez García, E. (Eds.), Pre-Mesozoic Geology of Iberia. Springer-Verlag, Berlin, pp. 92–102.

Pimentel, M.M., Whitehouse, M.J., Viana, M.G., Fuck, R.A., Machado, N., 1997. The Mara Rosa arc in the Tocantins province: further evidence for Neoproterozoic crustal accretion in central Brazil. Precambrian Research 81, 299–310.

Pin, C., Ortega Cuesta, L.A., Gil Ibarguchi, J.I., 1992. Mantle-derived, early Paleozoic A-type metagranitoids from the NW Iberian Massif: Nd isotope and trace-element constraints. Bulletin de la Societé Géologique de France 163, 483–494.

Pin, C., Paquette, J.L., Santos Zalduegui, J.F., Gil Ibarguchi, J.I., 2002. Early Devonian supra-subduction zone ophiolite related to incipient collisional processes in the Western Variscan Belt: the Sierra de Careón unit, Ordenes Complex, Galicia. In: Martínez Catalán, J.R., Hatcher, R.D., Arenas, R., Díaz García, F. (Eds.), Variscan–Appalachian Dynamics: the building of the Late Paleozoic basement: Geological Society of America Special Paper, vol 364, pp. 57–72.

Pin, C., Paquette, J.L., Ábalos, B., Santos, F.J., Gil Ibarguchi, J.I., 2006. Composite origin of an early Variscan transported suture: ophiolitic units of the Morais Nappe Complex (north Portugal). Tectonics 25, TC5001. doi:10.1029/2006TC001971.

Potrel, A., Peucat, J.J., Fanning, C.M., 1998. Archean crustal evolution of the West African Craton: example of the Amsaga Area (Reguibat Rise). U–Pb and Sm–Nd evidence for crustal growth and recycling. Precambrian Research 90, 107–117.

Ribeiro, M.L., Floor, P., 1987. Magmatismo peralcalino no Maciço Hespérico: sua distribução e significado geodinámico. In: Bea, F., Carnicero, A., Gonzalo, J.C., López-Plaza, M., Rodríguez Alonso, M.D. (Eds.), Geología de los granitoides y rocas asociadas del Macizo Hespérico. Rueda, Madrid, pp. 211–221.

Rocci, G., Bronner, G., Deschamps, M., 1991. Crystalline basement of the West African Craton. In: Dallmeyer, R.D., Lécorché, J.P. (Eds.), The West African orogens and circum-Atlantic correlatives. Springer-Verlag, Heidelberg, Germany, pp. 31–61.

Rodríguez, J., 2005. Recristalización y deformación de litologías supracorticales sometidas a metamorfismo de alta presión (Complejo de Malpica-Tuy, NO del Macizo Ibérico). Laboratorio Xeolóxico de Laxe, Nova Terra 29, 1–572.

Rodríguez Alonso, M.D., Peinado, M., López-Plaza, M., Franco, P., Carnicero, A., Gonzalo, J.C., 2004. Neoproterozoic–Cambrian synsedimentary magmatism in the Central Iberian Zone (Spain): geology, petrology and geodynamic significance. International Journal of Earth Sciences 93, 897–920.

Rodríguez, J., Cosca, M.A., Gil Ibarguchi, J.I., Dallmeyer, R.D., 2003. Strain partitioning and preservation of 40Ar/39Ar ages during Variscan exhumation of a subducted crust (Malpica-Tui complex, NW Spain). Lithos 70, 111–139.

Rodríguez, J., Paquette, J.L., Gil Ibarguchi, J.I., 2007. U–Pb dating of Lower Ordovician alkaline magmatism in the Gondwana margin (Malpica-Tui complex, Iberian Massif): latest continental events before oceanic spreading. In: Arenas, R., Martínez Catalán, J.R., Abati, J., Sánchez Martínez, S. (Eds.), IGCP 497: The Rheic ocean: its origin, evolution and correlatives, A Coruña, Spain, The rootless Variscan suture of NW Iberia (Galicia, Spain), Field trip guide & Conference abstracts, pp. 163–164.

Rolet, J., Gresselin, F., Jegouzo, P., Ledru, P., Wyns, R., 1994. Intracontinental Hercynian events in the Armorican Massif, structure and metamorphism, the Variscan orogeny in the Armorican Massif. In: Keppie, J.D. (Ed.), Pre-Mesozoic geology in France and related areas. Springer-Verlag, Berlin, Germany, pp. 195–215.

Sánchez Martínez, S., 2009. Geoquímica y geocronología de las ofiolitas de Galicia. Laboratorio Xeolóxico de Laxe. Nova Terra 37, 1–351.

Sánchez Martínez, S., Jeffries, T., Arenas, R., Fernández-Suárez, J., García-Sánchez, R., 2006. A pre-Rodinian ophiolite involved in the Variscan suture of Galicia (Cabo Ortegal Complex, NW Spain). Journal of the Geological Society 163, 737–740.

Sánchez Martínez, S., Arenas, R., Díaz García, F., Martínez Catalán, J.R., Gómez-Barreiro, J., Pearce, J.A., 2007. Careón ophiolite, NW Spain: suprasubduction zone setting for the youngest Rheic Ocean floor. Geology 35, 53–56.

Santos Zalduegui, J.F., Schärer, U., Gil Ibarguchi, J.I., 1995. Isotope constraints on the age and origin of magmatism and metamorphism in the Malpica-Tuy allochthon, Galicia, NW Spain. Chemical Geology 121, 91–103.

Santos, J.O.S., Hartmann, L.A., Gaudette, H.E., Groves, D., McNaughton, N.J., Fletcher, I.R., 2000. A new understanding of the provinces of the Amazon craton based on integration of field mapping and U–Pb and Sm–Nd geochronology. Gondwana Research 3, 453–488.

Santos, J.F., Schärer, U., Gil Ibarguchi, J.I., Girardeau, J., 2002. Genesis of pyroxenite-rich peritotite at Cabo Ortegal (NW Spain): geochemical and Pb–Sr–Nd isotope data. Journal of Petrology 43, 17–43.

Santos, T.J.S., Fetter, A.H., Neto, J.A.N., 2008. Comparisons between the northwestern Borborema Province, NE Brazil, and the southwestern Pharusian Dahomey Belt, SW Central Africa. In: Pankhurst, R.J., Trouw, R.A.J., Brito-Neves, B.B., de Wit, M.J. (Eds.), West Gondwana: pre-Cenozoic correlations across the South Atlantic Region: Geological Society of London Special Publication, vol 294, pp. 101–119.

Shelley, D., Bossière, G., 2000. A new model for the Hercynian orogen of Gondwanan France and Iberia. Journal of Structural Geology 22, 757–776.

Shelley, D., Bossière, G., 2002. Megadisplacements and the Hercynian orogen of Gondwanan France and Iberia. In: Martínez Catalán, J.R., Hatcher, R.D., Arenas, R., Díaz García, F. (Eds.), Variscan-Appalachian dynamics: The building of the Late Paleozoic basement, Boulder, Colorado: Geological Society of America Special Paper, vol 364, pp. 209–222.

Stacey, J.S., Kramers, J.D., 1975. Approximation of terrestrial lead isotope evolution by a two-stage model. Earth and Planetary Science Letters 26, 207–221.

Stampfli, G.M., Borel, G.D., 2002. A plate tectonic model for the Paleozoic and Mesozoic constrained by dynamic plate boundaries and restored synthetic oceanic isochrones. Earth and Planetary Sciences Letters 196, 17–33.

Stampfli, G.M., von Raumer, J.F., Borel, G.D., 2002. Paleozoic evolution of pre-Variscan terranes: from Gondwana to the Variscan collision. In: Martínez Catalán, J.R., Hatcher, R.D., Arenas, R., Díaz García, F. (Eds.), Variscan–Appalachian dynamics: the building of the late Paleozoic basement, Boulder, Colorado: Geological Society of America Special Paper, vol 364, pp. 263–280.

Stern, R.J., 2008. Neoproterozoic crustalgrowth: the solid Earth system during a critical episode of Earth history. Gondwana Research 14, 33–50.

Ugidos, J.M., Bilström, K., Valladares, M.I., Barba, P., 2003a. Geochemistry of the Upper Neoproterozoic and Lower Cambrian siliciclastic rocks and U–Pb dating on detrital zircons in the Central Iberian Zone, Spain. International Journal of Earth Sciences 92, 661–676.

Ugidos, J.M., Valladares, M.I., Barba, P., Ellam, R.M., 2003b. The Upper Neoproterozoic–Lower Cambrian of the Central Iberian Zone, Spain: chemical and isotopic (Sm–Nd) evidence that the sedimentary succession records an inverted stratigraphy of its source. Geochimica et Cosmochimica Acta 67, 2615–2629.

Valverde-Vaquero, P., Dunning, G.R., 2000. New U–Pb ages for Early Ordovician magmatism in central Spain. Journal of the Geological Society 157, 15–26.

Valverde-Vaquero, P., Marcos, A., Farias, P., Gallastegui, G., 2005. U–Pb dating of Ordovician felsic volcanism in the Schistose Domain of the Galicia-Trás-os-Montes Zone near Cabo Ortegal (NW Spain). Geologica Acta 3, 27–37.

Van Staal, C.R., De Roo, J.A., 1995. Mid-Paleozoic tectonic evolution of the Appalachian central mobile belt in northern New Brunswick, Canada: collision, extensional collapse and dextral transpression. In: Hibbard, J.P., Van Staal, C.R., Cawood, P.A. (Eds.), Current perspectives in the Appalachian–Caledonian orogen, St. John's, Newfoundland: Geological Association of Canada Special Paper, vol 41, pp. 367–389.

von Raumer, J.F., Stampfli, G.M., 2008. The birth of the Rheic Ocean—Early Palaeozoic subsidence patterns and subsequent tectonic plate scenarios. Tectonophysics 461, 9–20.

von Raumer, J.F., Stampfli, G.M., Bussy, F., 2003. Gondwana-derived microcontinents—the constituents of the Variscan and Alpine collisional orogens. Tectonophysics 365, 7–22.

Walker, J.D., Geissman, J.W., 2009. Geologic Time Scale: Geological Society of America. doi:10.1130/2009.CTS004R2C. compilers.

Winchester, J.A., Pharaoh, T.C., Verniers, J., 2002. Palaeozoic amalgamation of central Europe: an introduction and synthesis of new results from recent geological and geophysical investigations. In: Winchester, J.A., Pharaoh, T.C., Verniers, J. (Eds.), Palaeozoic amalgamation of central Europe, London: Geological Society of London Special Publication, vol. 201, pp. 1–18.